
Influence of hydrostratigraphy and structural setting on the arsenic occurrence in groundwater of the Cimino-Vico volcanic area (central Italy)

Massimo Angelone · Carlo Cremisini ·
Vincenzo Piscopo · Marco Proposito · Fabio Spaziani

Abstract Arsenic occurrence in groundwater near the Cimino-Vico volcanoes (central Italy) was analysed considering the hydrostratigraphy and structural setting and the shallow and deep flows interacting within the Quaternary volcanics. Groundwater is the local source of drinking water. As documented in the past, arsenic in the groundwater has become a problem, and the European maximum allowable contaminant level was recently lowered to 10 µg/L. Chemical analyses of groundwater were conducted, sampled over an area of about 900 km², from 65 wells and springs representative of the volcanic aquifer and thermal waters. Considering the type of aquifer, the nature of the aquifer formation and its substratum, the hydrochemical data highlight that the arsenic content of the groundwater is mainly connected with the hydrothermal processes in the volcanic area. Thermal waters (54–60°C) fed from deep-rising fluids show higher arsenic concentrations (176–371 µg/L). Cold waters sampled from the volcanic aquifer are characterized by a wide variability in their arsenic concentration (1.6–195 µg/L), and about 62% exceed the limit of 10 µg/L. Where the shallow volcanic aquifer is open to deep-rising thermal fluids, relatively high arsenic concentrations (20–100 µg/L) are found. This occurs close to areas of the more recent volcano-tectonic structures.

Keywords Arsenic · Italy · Volcanic aquifer · Hydrochemistry · General hydrogeology

Introduction

Arsenic contamination of drinking water is a subject of high environmental concern. In the last several years, numerous papers have focused on this matter, particularly the massive episodes of severe arsenic poisoning that occurred in the Bengal basin (Anawar et al. 2002; Rahman et al. 2005). Other well-known incidents have been reported in Taiwan, Chile, and Argentina (Mandal and Suzuki 2002). In Europe and in the USA, several episodes concerning the presence of arsenic in drinking waters have been recently reported (Nordstrom 2002; Čavar et al. 2005; Gómez et al. 2006; Kelepertsis et al. 2006; Meliker et al. 2006).

This worldwide attention is related to the acute long-term health effects observed in populations exposed to arsenic-rich drinking waters. Epidemiological studies have shown that arsenic can cause a number of different illnesses, especially skin, lung, and bladder cancer (Karim 2000; Rossman et al. 2004; Tchounwou et al. 2004; Yoshida et al. 2004).

From a toxicological point of view, the poisoning qualities of arsenic depend on the chemical form and oxidation state in which it is present in the water (Mandal and Suzuki 2002; Bhattacharyya et al. 2003). The predominant dissolved arsenic species in groundwater are the trivalent (AsIII) and pentavalent (AsV) inorganic forms (Plant et al. 2005), but the As(III) compounds are more toxic than the As(V) ones (Jain and Ali 2000; Hughes 2002). Until now, the various forms of arsenic have not been discriminated in the evaluation of water quality, with only total arsenic considered for the maximum contaminant level in drinking water (Kim et al. 2002).

The occurrence of arsenic in groundwater can derive from either anthropogenic causes such as mining (Morin and Calas 2006), or natural causes. For public health, contamination from natural causes is more difficult to characterize and manage, being generally due to non-point

Received: 12 March 2008 / Accepted: 3 November 2008
Published online: 4 December 2008

© Springer-Verlag 2008

Electronic supplementary material The online version of this article (doi:10.1007/s10040-008-0401-3) contains supplementary material, which is available to authorized users.

M. Angelone · C. Cremisini · M. Proposito
ENEA-CR Casaccia, ACS,
Via Anguillarese 301, 00123, Rome, Italy

V. Piscopo (✉) · F. Spaziani
Dept. Ecologia, e Sviluppo Economico Sostenibile,
Università della Tuscia,
Via S. Giovanni Decollato 1, 01100, Viterbo, Italy
e-mail: piscopo@unitus.it

sources. Usually, the natural occurrence of arsenic in groundwater is related to the presence of geothermal systems (Ballantyne and Moore 1988; Webster and Nordstrom 2003) or to water–rock interactions that lead to arsenic mobilization from the aquifer, both in reducing and oxidizing environments, under specific geochemical and stratigraphical conditions (Smedley and Kinniburgh 2002; Charlet and Polya 2006). In the volcanic areas of southern Italy, high arsenic concentrations have been related to the deep-rising fluids of the active geothermal systems (Aiuppa et al. 2003).

In Europe, following the recent legislative revision concerning the quality standards for drinking waters (98/83 EC Directive 1998), arsenic is now not only a health problem but also a socioeconomic problem. The maximum allowable concentration level has been lowered from 50 to 10 $\mu\text{g/L}$, and, as a consequence, several local public administrators and water management companies must invest money in order to ensure drinking resources in accordance with the new rules.

The purpose of this report is to provide a hydrogeological interpretation of arsenic occurrence in groundwater of the Cimino-Vico volcanic area in central Italy. Though the presence of minor toxic elements in the groundwater of this area has been documented for about 30 years (Cremisini et al. 1979; Dall'Aglio et al. 2001; Mari et al. 2006; Vivona et al. 2007), several villages are now involved in the arsenic-related emergency as a result of the new concentration limit. It is essential, therefore, to characterize in detail the relations between arsenic, hydrochemistry, and hydrogeology. In this study, the occurrence of arsenic in groundwater is considered at the scale of the volcanic system to evaluate hydrostratigraphical and structural controls on arsenic concentration in groundwater used as the source of drinking water by about 150,000 local inhabitants. This understanding is important to address the future options for groundwater resource management, all the more because groundwater in the wider volcanic region of northern Latium, which includes the Cimino-Vico system, supplies about 6 m^3/s of drinking water.

Geological outline

The area investigated comprises the Cimino and Vico volcanic complexes (Fig. 1) and covers a surface area of some 900 km^2 . Although situated in the same volcanic region (Roman Province), the Cimino and Vico complexes belong to separate magmatic series: potassic series and high-potassium series, respectively (Appleton 1972; Marinelli 1975; Peccerillo and Manetti 1985; Beccaluva et al. 1991; Conticelli and Peccerillo 1992).

The Cimino complex was active between 1.35 and 0.95 million years ago (Ma). Effusive and explosive activity gave rise to several domes developed along NW–SE and NE–SW fractures and included some pyroclastic flows and pyroclastic surges. During the final cycle, a central volcano developed. The products of the Cimino complex

are mainly composed of latites and trachytes (Sollevanti 1983; Lardini and Nappi 1987).

The Vico complex is situated immediately south of the Cimino volcanic complex and consists of a strato-volcano with a central caldera depression housing Lake Vico (Fig. 1). The Vico Volcano was active between 419,000 years ago (ka) and 95 ka and developed on a graben elongated NW–SE at the intersection with a NE–SW fracture. Alternating explosive and effusive phases characterized the volcanic history with the formation of several plinian fall deposits, lava flows, and pyroclastic flows, followed at the end by circum-caldera hydro-magmatic and Strombolian eruptions. The products of Vico Volcano are mainly leucitites, phono-tephrites and leucite-phonolites (Locardi 1965; Mattias and Ventriglia 1970; Bertagnini and Sbrana 1986; Perini et al. 1997; Nappi et al. 2004). The volcanic rocks are covered and bounded locally by Pleistocene-Holocene continental sediments consisting of alluvial sandy-silty deposits, as well as travertine deposits (Fig. 1).

The substratum beneath the Cimino and Vico volcanics consists of sedimentary rocks: a Pliocene-Pleistocene sedimentary complex, including conglomerates, sandstones, sands, and clays; the Upper Cretaceous-Oligocene Flysch (Ligurian Units), consisting of alternating calcareous-pelitic-calcareous and arenaceous-pelitic-turbidites; the Triassic-Palaeogene carbonate rocks (Tuscan-Umbrian-Marche Units), several thousand meters thick, including limestones, marly limestones, marls, dolomitic limestones, dolostone, and anhydrites (Baldi et al. 1974; Funicello et al. 1977; La Torre et al. 1981; Buonasorte et al. 1991).

The structural features of the area are very complex because of neotectonic activity and more recent volcano-tectonic related deformation. Within the study area, faults oriented N–S, E–W, NW–SE and NE–SW subdivide the deep structures and control the uplift of the volcanic basement (Baldi et al. 1974). This results in a relatively shallow depth of the volcanic basement near the town of Viterbo. Meanwhile, the volcanic complexes overlay the Pliocene-Pleistocene sedimentary complex in the eastern zone and the Upper Cretaceous-Oligocene Flysch in the western zone along a NW–SE oriented strip where the thermal springs of Viterbo emerge (Fig. 1).

Hydrogeology

The Cimino and Vico volcanics constitute an aquifer system limited by the Pliocene-Pleistocene sedimentary complex on its eastern edge and by the Upper Cretaceous-Oligocene Flysch on its western and south-western sides, as shown in Fig. 2. A continuous basal aquifer, as well as several perched aquifers of limited, discontinuous extent, has been found (Boni et al. 1986; Capelli et al. 2005; Baiocchi et al. 2006).

The basal aquifer is characterized by radially divergent flow, which is controlled by the boundaries of the Pliocene-Pleistocene sedimentary complex along the

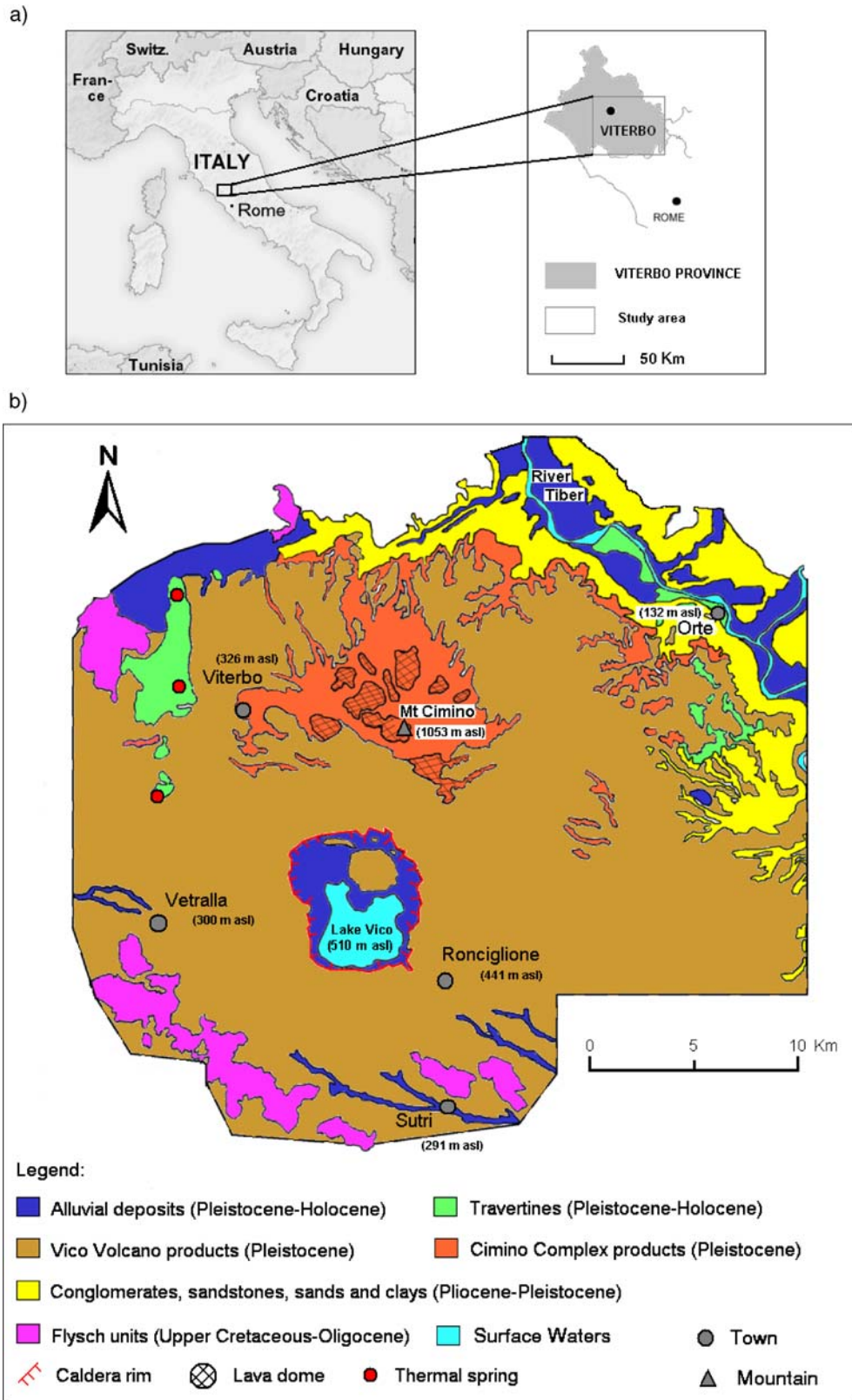


Fig. 1 a Location map of the Cimino-Vico volcanic area, and b surface geology of the study area (modified from Sollevanti 1983)

north-eastern margin, and by the Upper Cretaceous-Oligocene Flysch along the south-western and north-western margins (Fig. 2). The potentiometric surface follows the topography, especially in the central sector,

which includes the Cimino domes and the Lake Vico caldera, where the morphological high corresponds to the piezometric high, as shown in Fig. 2. In this area, the effect of the lake on groundwater flow is quite evident,

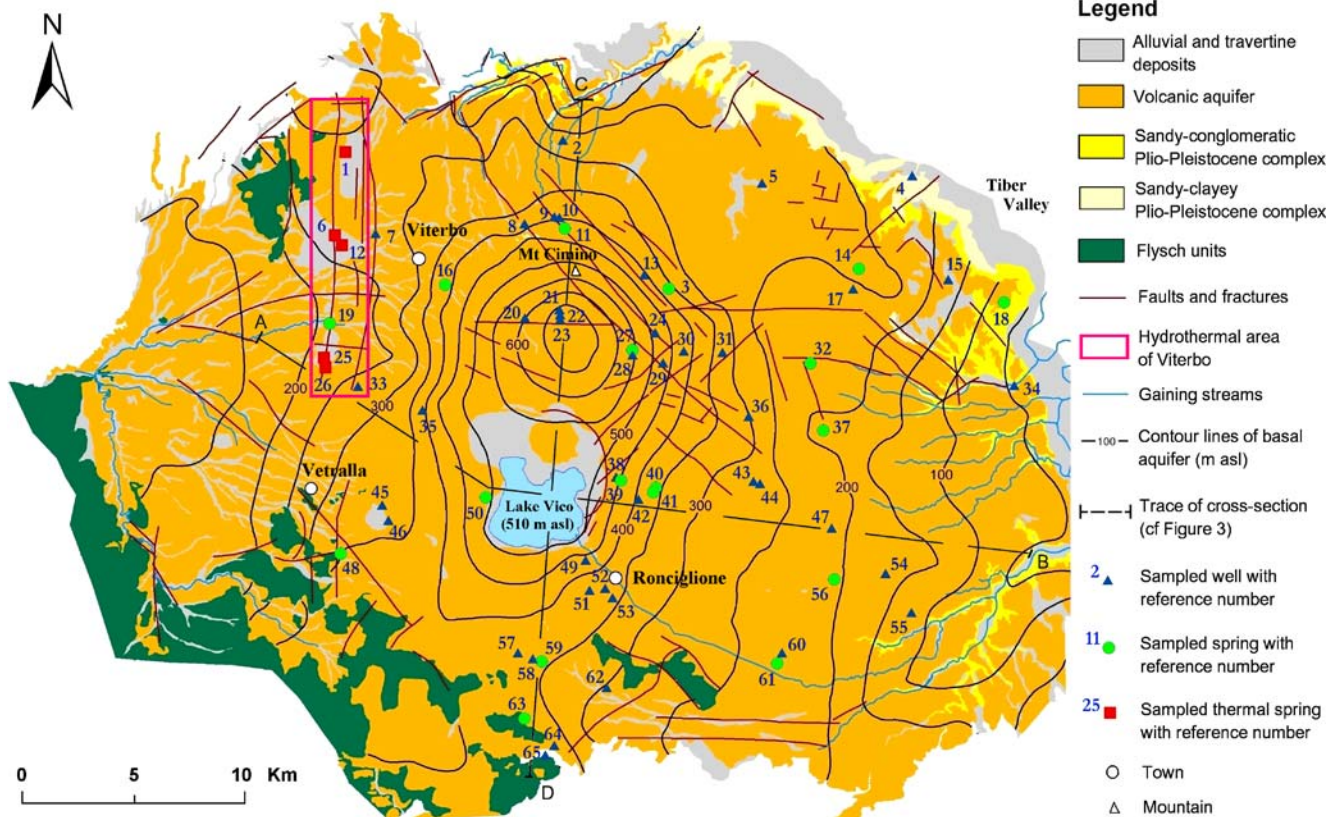


Fig. 2 Simplified surface geology and potentiometric surface of the basal aquifer in the Cimino-Vico volcanic area (modified from Baiocchi et al. 2006) with location of the wells and springs sampled

with the surface of the lake related to that of the basal unconfined aquifer (Baiocchi et al. 2006).

The volcanic aquifer discharges mainly into the streams of the eastern, south-eastern, western, and northern slopes and also from springs (generally with flow of not more than a few tens of litres per second). Most of the springs are related to the perched aquifers. Groundwater outflow from the volcanic aquifer towards the alluvial aquifer of the Tiber Valley has been found in the south-eastern boundary of the volcanites, where the Pliocene-Pleistocene sedimentary complex is made up of sandy-conglomeratic deposits (Baiocchi et al. 2006).

The central portion of the system, including the Cimino domes and the Vico Lake caldera, is characterized by the lowest transmissivity values, generally between 10^{-6} and 10^{-4} m²/s. Towards the marginal zones to the W and SE, where the main discharge areas are situated, the aquifer transmissivity values are higher, generally between 10^{-4} and 10^{-2} m²/s (Baiocchi et al. 2006).

The mean groundwater yield of the volcanic aquifer has been estimated between 5 and 7 m³/s. The discharge of the volcanic aquifer has been estimated at about 2.0 m³/s in the streams and springs, about 2.3 m³/s as flow towards adjacent aquifers, and about 1.5 m³/s pumped from numerous and scattered wells that supply the local drinking water and irrigation needs (Baiocchi et al. 2006).

In the studied area, a second aquifer has been identified at depth, consisting primarily of the Triassic-Palaeogene carbonate rocks, which host a thermal reservoir. The shallow volcanic aquifer and the deep aquifer are separated by a great thickness of low-permeability Pliocene-Pleistocene and Upper Cretaceous-Oligocene sedimentary rocks. West of Viterbo, the volcanic basement has been uplifted, and the Upper Cretaceous-Oligocene Flysch has a relatively reduced thickness and is fractured and faulted, as shown in Fig. 3. These last conditions enable the uprising of thermal waters which feed several springs and deep wells (Fig. 2). Thermal waters with temperatures between 50 and 64°C, of the sulphate-alkaline-earth type, are more mineralized (electrical conductivity between 2,700 and 3,400 μS/cm) and have higher gas contents (CO₂ and H₂S). In contrast, the waters of the volcanic aquifer comprise fresh (electrical conductivity between 200 and 900 μS/cm) and cold waters (temperature between 13 and 20°C) of the bicarbonate-alkaline-earth type (Piscopo et al. 2006).

The recharge area for the thermal system corresponds to the morphological high between the Cimino domes and the Vico Caldera; it is here that, due to the presence of deep volcano-tectonic fractures, infiltrations are diverted to recharge both the shallow volcanic aquifer and the deep aquifer. The yield of the deep aquifer for

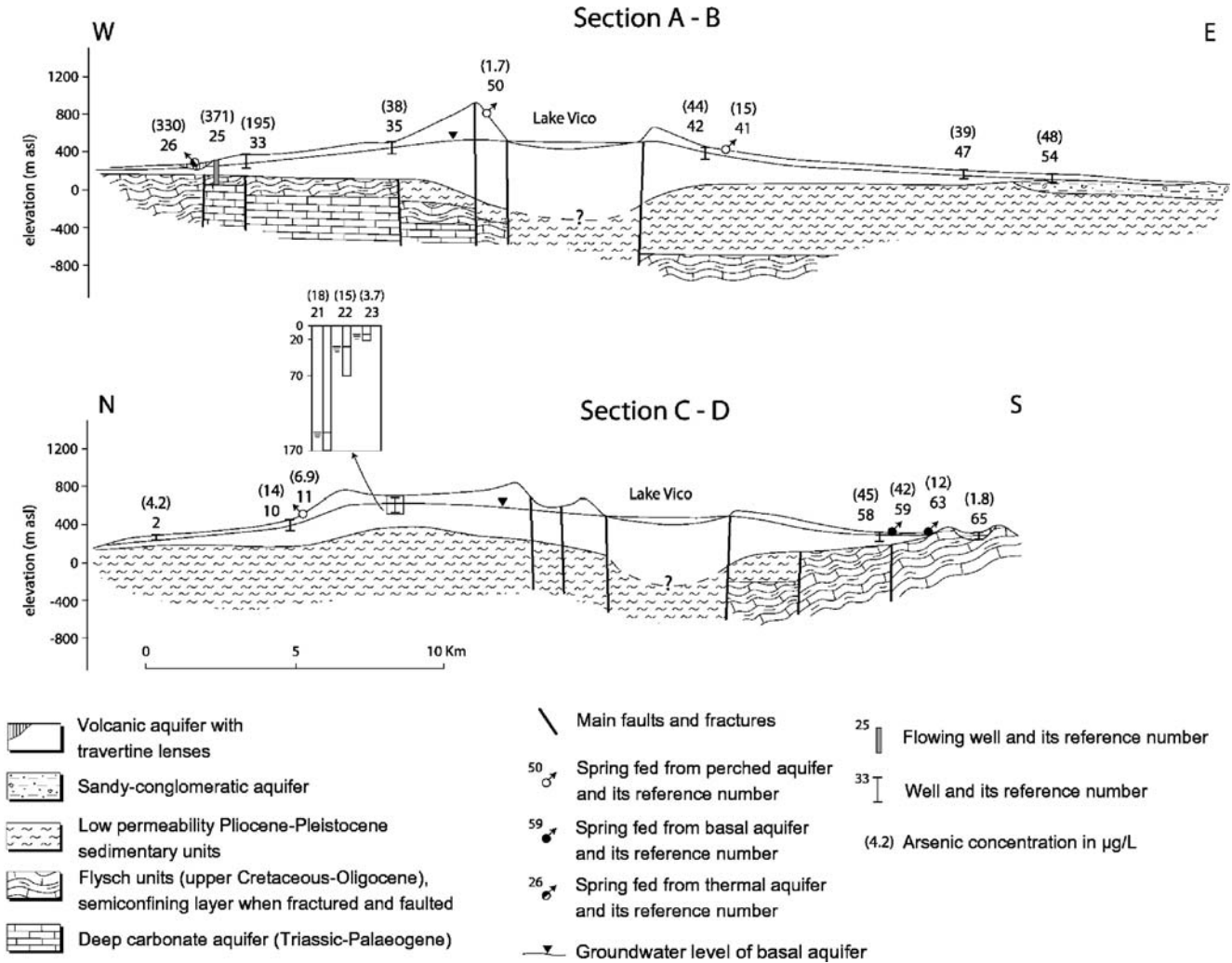


Fig. 3 Simplified hydrogeological cross-sections through Cimino-Vico volcanoes (A–B and C–D in Fig. 2) including some wells and springs with As concentrations in groundwater. The geology is derived from Baldi et al. (1974), La Torre et al. (1981), and Buonasorte et al. (1991)

the thermal area of Viterbo is around 0.1 m³/s (Piscopo et al. 2006).

Materials and methods

Water from a total of 65 different sources, including 43 wells and 22 springs, was sampled during a survey carried out from March to September 2007. The wells tap the basal aquifer (40 wells), perched aquifers (2 wells), and thermal water (1 well). The springs are fed from the basal aquifer (6 springs), perched aquifers (12 springs), and geothermal system (4 springs). The elevations above sea level of the springs and the groundwater level in wells compared with those of the continuous basal aquifer, as well as the local hydrostratigraphy, the flow rate of springs, and the yield and depth of wells, enables one to distinguish between the basal and perched aquifers. The available data are summarized in Table 1 for the wells and springs sampled.

The sampling points were selected considering a homogeneous coverage of the investigated area (Fig. 2), a representative sample of groundwater source types, and the wells and springs that supply the local drinking water. The groundwater samples were collected in polyethylene bottles, pre-cleaned in the laboratory with 1:3 diluted HNO₃, and then thoroughly rinsed with ultra-pure deionized water. The wells were pumped for a long time, in order to remove stagnant water from the pipes, at a flow rate of a maximum of a few liters per second, ensuring a reduced drawdown in the penetrated saturated thickness.

Temperature (T), pH, Eh, and electrical conductivity (EC) were measured in the field using portable meters equipped with sensors and electrodes. All meters were calibrated and tested daily before the measurements. Each water sample was filtered with a 0.45-µm Teflon filter and divided into two parts. The first part was acidified to pH<2 with HNO₃ (BDH-Aristar grade) and saved for the determination of major cations and trace elements, while the second was kept for anion determination. All the samples were immediately stored at 4°C until the

Table 1 Summary of the main characteristics of the wells (*top half*) and springs (*bottom half*) sampled

Wells Number of wells	Aquifer formation tapped by well	Aquifer substratum	Aquifer type	Range of depth (m)	Range of flow rate (L/s)
3	Sandy-conglomeratic and alluvial deposits	Plio-Pleistocene sandy-clayey deposits	Basal aquifer	20–80	1–6
14	Cimino volcanites and sandy-conglomeratic deposits	Plio-Pleistocene sandy-clayey deposits	Basal aquifer	50–210	0.2–15
2	Cimino volcanites	Upper Cretaceous-Oligocene Flysch	Perched aquifer	10–70	0.1–0.3
11	Vico volcanites		Basal aquifer	30–170	1–12
12	Vico volcanites and sandy-conglomeratic deposits	Plio-Pleistocene sandy-clayey deposits	Basal aquifer	40–300	2–10
1	Volcanites and Flysch	Upper Cretaceous-Oligocene Flysch	Deep confined aquifer	130	10
Springs					
Number of springs	Aquifer formation	Aquifer type	Range of elevation (m asl)	Range of flow rate (L/s)	
1	Sandy-conglomeratic deposits	Perched aquifer	200	4	
4	Cimino volcanites	Perched aquifer	390–600	2–8	
7	Vico volcanites	Perched aquifer	230–650	0.1–5	
6	Vico volcanites	Basal aquifer	170–350	2–20	
4	Hydrothermal system	Deep confined aquifer	230–320	1–6	

laboratory analyses. Field blanks were also prepared, for a total of 16, using ultra-pure deionized water manipulated with the same procedures and equipment as the samples.

Major anions (HCO_3^- , Cl^- , SO_4^{2-}), nitrate (NO_3^-), fluoride (F^-), and bromide (Br^-) were measured in the laboratory within 24 hours of sample collection. HCO_3^- was determined by means of titration, using HCl 0.01N as a titrant and methyl-orange as a pH indicator. F^- , Cl^- , Br^- , NO_3^- , and SO_4^{2-} were determined by ion chromatography (IC) using a Dionex-DX-120 system.

Major cations (Na^+ , K^+ , Ca^{2+} , Mg^{2+}), Fe, and SiO_2 were determined with an ICP-OES (Perkin-Elmer OPTIMA 2000 DV), whereas an ICP-MS (Perkin-Elmer ELAN 6100) was employed for the trace element analyses (As, B, Ba, Mn, Rb, Sb, Sr, U, V).

The data quality control was performed in three phases: analyses of field blanks, analyses of certified reference materials (CRM), and analyses of sample replicates. The results obtained on the 16 field blanks assured that no contamination occurred during the sampling.

Three CRM were used to test the accuracy and precision of the results: SRM-1640 (a natural fresh water provided by NIST, National Institute of Standards and Technology), BCR-609, and BCR-610 (two groundwater samples supplied by IRMM, Institute for Reference Materials and Measurements). The values found in the laboratory, as the mean and standard deviation of 10 replicates, are in very good agreement with the certified values ($\pm 2\%$).

Ten randomly selected samples were replicated three times during different sessions, in order to verify the reproducibility of the data. This indicated a variability of less than $\pm 1\%$. The ionic balance was checked for all the samples using AQUACHEM 5.1 software. The mean deviation from

the electroneutrality, calculated on the absolute value of the resulting percentages, was $1.8\% \pm 1.3\%$.

Results

A summary of the chemical analyses is given in Table 2 and the full dataset is given as Electronic supplementary material (see Table 1 of Electronic supplementary material).

Since the major constituents of some waters were also determined in a previous investigation (Piscopo et al. 2006), the results obtained in the present study were compared with the former data, in order to evaluate each time-related variation in the chemical compositions, but no significant differences were identified.

Based on the relative amount of major ions, the temperature, and the salinity, the sampled waters can be subdivided into two main groups (Table 2): thermal (5 samples) and cold waters (60 samples). Thermal waters (samples numbered 1, 6, 12, 25, and 26 in Fig. 2) with CaSO_4 chemical composition show relatively high mineralization ($\text{EC} = 2780\text{--}3230 \mu\text{S/cm}$) and temperature ($T = 54\text{--}60^\circ\text{C}$). These characteristics are related to the deep groundwater circulation in the volcanic basement flowing from springs and in deep wells located in the area where the volcanic substratum is uplifted, fractured, and faulted (Piscopo et al. 2006).

Cold waters with Ca-HCO_3 chemical compositions tending towards an alkaline-bicarbonate type show low salinity ($\text{EC} = 123\text{--}749 \mu\text{S/cm}$, except sample no. 4 in Fig. 2, which corresponds to a contaminated well in the alluvial plain of the Tiber River) and low temperature ($T = 7\text{--}22^\circ\text{C}$). These waters are those sampled from wells and springs in the volcanic aquifer and its adjacent

Table 2 Descriptive statistics summary of the chemical analyses on the sampled waters. *SD* standard deviation

Thermal waters						Cold waters					
	Unit	Mean	Median	Minimum	Maximum	SD	Mean	Median	Minimum	Maximum	SD
As	µg/L	305	329	176	371	75	23	15	1.6	195	28
U	µg/L	0.07	0.07	0.06	0.09	0.01	7.2	3.2	0.04	49	9.8
V	µg/L	0.69	0.73	0.28	0.95	0.28	9.4	9.5	0.09	23	5.2
Sb	µg/L	0.01	0.01	0.01	0.01	0.00	0.67	0.57	0.02	1.8	0.45
Rb	µg/L	130	130	124	135	4.6	84	59	19	386	69
Sr	µg/L	15,506	15,273	14,441	16,725	937	291	212	57	1,207	221
Ba	µg/L	38	36	35	44	3.8	39	9.9	0.64	547	93
B	µg/L	1,001	964	939	1,107	70	232	146	39	946	194
Fe	µg/L	13	3.9	3.3	50	20	25	4.8	0.44	396	61
Mn	µg/L	19	16	14	27	5.3	17	0.30	0.06	573	80
Ca ²⁺	mg/L	596	561	530	690	78	33	22	7.9	179	34
Mg ²⁺	mg/L	144	141	122	160	15	8.3	7.7	3.4	29	4.4
Na ⁺	mg/L	32	32	32	33	0.61	19	17	7.9	37	6.6
K ⁺	mg/L	30	29	28	31	1.4	15	16	1.4	37	9.6
F ⁻	mg/L	2.8	2.8	2.6	3.0	0.17	0.59	0.38	0.05	4.2	0.65
Cl ⁻	mg/L	12	12	11	13	0.49	17	13	7.5	45	9.0
Br ⁻	µg/L	56	60	10	90	30	68	64	24	188	26
NO ₃ ⁻	mg/L	0.00	0.00	< 0.1	< 0.1	0.00	14	11	0.10	54	13
SO ₄ ²⁻	mg/L	1,369	1,320	1,080	1,600	218	14	8.9	2.3	162	23
HCO ₃ ⁻	mg/L	969	1,018	786	1,037	105	159	120	44	550	98
SiO ₂	mg/L	24	23	22	27	1.9	30	30	12	46	7.3
T	°C	57	57	54	60	2.2	17	17	7.0	22	2.4
EC	µS/cm	2,978	2,870	2,780	3,230	224	330	289	123	1,065	168
pH		7.0	6.6	6.4	8.1	0.72	7.0	7.1	5.8	7.9	0.43
Eh	mV	-118	-138	-181	9.7	74	314	310	175	530	78

sedimentary aquifers (i.e. sandy-conglomeratic and alluvial aquifers).

The two main groups of waters show differences in the concentration of the minor and trace constituents, as well. A nitrate concentration lower than 0.1 mg/L characterizes the thermal waters, while variable values up to 54 mg/L were found for the cold waters, depending on the location of the sampled point with respect to intensive agricultural land use. The silica content of the thermal waters varies in a restricted range (22–27 mg/L), while a wider range (15–46 mg/L) was found for the cold waters due to the variable water interaction with the volcanic and Quaternary

sedimentary rocks. The cold waters are richer in uranium (0.04–49 µg/L) than the thermal waters (0.06–0.09 µg/L). The highest uranium concentrations (10–49 µg/L) are associated with the younger volcanic products of the Vico Volcano, where uranium mineralization in the alkaline volcanic deposits has been documented (Locardi 1967, 1973). In addition, the other minor and trace elements show significant variations, including the arsenic content.

The cold waters show a wide variability in arsenic concentration, and 37 samples (about 62%) exceed the limit of 10 µg/L (Fig. 4). The thermal waters show higher arsenic concentrations (Fig. 4), as well as concentrations

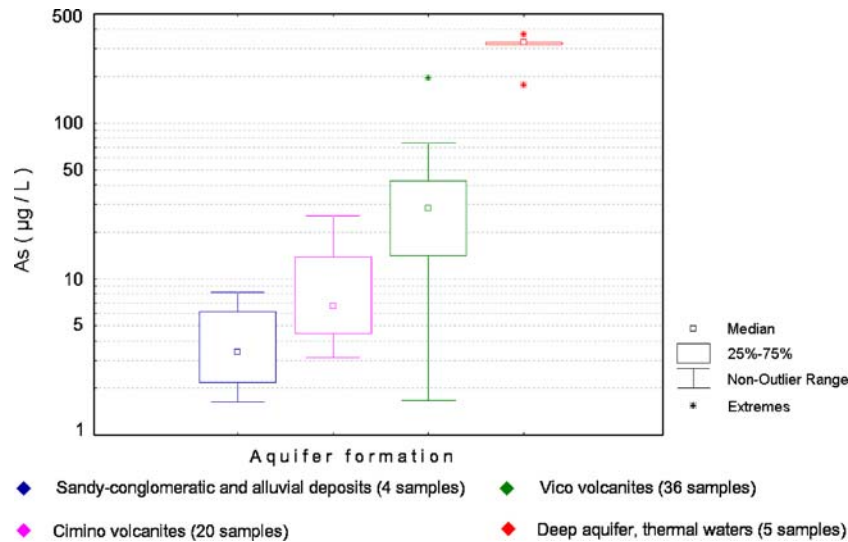


Fig. 4 Box plot showing As in groundwater and nature of the aquifer formation

of strontium, boron, and fluoride. The arsenic distribution in all the samples shows that the data are not normally distributed.

The Pearson correlation matrix calculated on the entire dataset (see Table 2 of Electronic supplementary material) shows that arsenic is strongly correlated with boron ($R=0.8$), fluoride ($R=0.9$), T ($R=0.9$), and EC ($R=0.9$). Even when the thermal waters are removed from the computation, the strong correlations of arsenic with boron ($R=0.7$) and fluoride ($R=0.9$) remain. The correlation matrix also highlights the relationship between arsenic and sulphate ($R=0.9$), which is mostly affected by thermal waters, since this correlation becomes very low when only the cold waters were considered.

Since arsenic, along with other measured parameters, is not normally distributed, the nonparametric Spearman correlation was also considered. Even in this case, the strong correlations of arsenic with boron ($R=0.8$) and fluoride ($R=0.8$), and a good correlation with temperature ($R=0.5$) and sulphate ($R=0.5$), are verified.

A first estimate of the dissolved arsenic species in the sampled waters can be deduced from the Eh-pH diagram shown in Fig. 5. Almost all of the samples are part of the arsenate domain (H_2AsO_4^- and HAsO_4^{2-}). The thermal waters (except one sampled far from the emerging point) fall instead in the arsenite domain (H_3AsO_3).

Saturation indices with respect to some mineral phases were calculated (see Table 3 of Electronic supplementary material) using the PHREEQC software (Parkhurst and Appelo 1999). The samples are supersaturated with respect to iron oxides and undersaturated with respect to most common As-bearing minerals. The samples of thermal waters and of the deep well from around the hydrothermal area near the town of Viterbo are in equilibrium or saturated with fluorite, and are those with the highest arsenic concentrations. Saturation indices of fluorite show a good correlation with arsenic concentration for all samples ($R=0.7$). The thermal waters and cold waters circulating in the Quaternary sedimentary aquifers

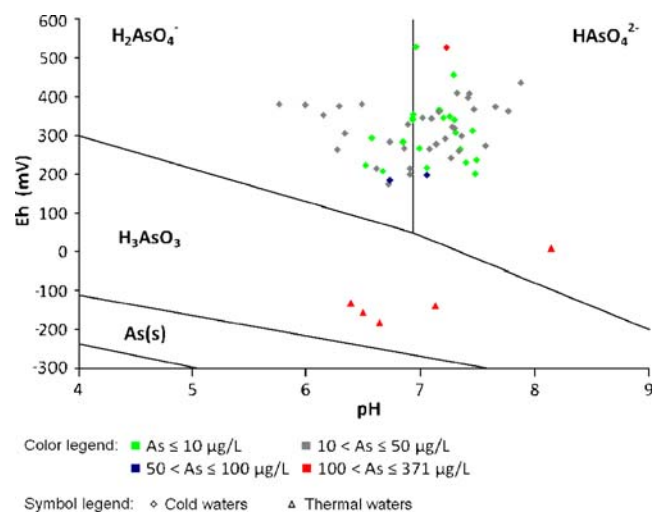


Fig. 5 Eh-pH diagram of As species showing As concentrations and type of water sampled

are the only samples saturated with respect to calcite, highlighting the interaction with the carbonate rocks (deep substratum of volcanics and conglomerates, respectively).

A multivariate statistical study, the principal component analysis (PCA), was performed using the STATISTICA software in order to better understand the intercorrelations of the chemical parameters. This computation reduces the dimensionality of the data by transforming a group of correlated variables into a smaller number of uncorrelated variables called principal components (Meglin 1991; Stetzenbach et al. 2001). The PCA was performed as an eigenanalysis of the correlation matrix; the data were standardized first, in order to assure an equal weight to the variables (Fitzpatrick et al. 2007), and the Varimax rotation was adopted to maximize the variation explained by the components (Reyment and Jvreskog 1996).

Six factors (with eigenvalues greater than 1) resulted from the computation, explaining about 82% of the variance in the dataset (see Table 4 of Electronic supplementary material); the factors correspond to the eigenvectors of the correlation matrix, and the eigenvalues correspond to the proportion of the variance explained by these factors. The principal component scores were successively calculated as linear combinations of the standardized data with the factor loadings (Farnham et al. 2000, 2003). Then, considering only the first three factors (about 63% of the variance) and plotting the related principal components scores (PC) on a three-dimensional diagram, four clusters were distinguished (Fig. 6). Group A, characterized by high PC1 scores, includes the thermal waters. Group B includes cold waters sampled from the volcanic aquifer with relatively high concentrations of As, B, F^- , and/or U. Group C includes cold waters characterized by relatively high concentrations of Ca^{2+} , HCO_3^- , Cl^- , and EC, and it corresponds to the wells and springs of the Quaternary sedimentary aquifers, and group D includes cold waters sampled from the volcanic aquifer that do not show combinations of extreme values for two or more variables.

The hydrochemical results were further considered to study the correlations between the distribution of arsenic in groundwater and type of aquifer, nature of aquifer formation, the aquifer substratum, and the depth of the well, based on the characteristics of each point sampled as reported in Table 1.

The highest arsenic concentrations are found close to the area where the thermal waters rise from the deep carbonate aquifer, as shown in Fig. 7. Values of arsenic concentration above $20 \mu\text{g/L}$ encircle the thermal area, extending along a zone oriented NW-SE. Here, the wells and springs sampled correspond mainly to the basal unconfined aquifer composed of Cimino and Vico volcanic products, overlaying the fractured and faulted Upper Cretaceous-Oligocene Flysch in the western sector of the system (Fig. 3). The waters of group B also fall in this zone.

Values of arsenic concentration lower than $20 \mu\text{g/L}$ characterize the north-eastern and south-western zones

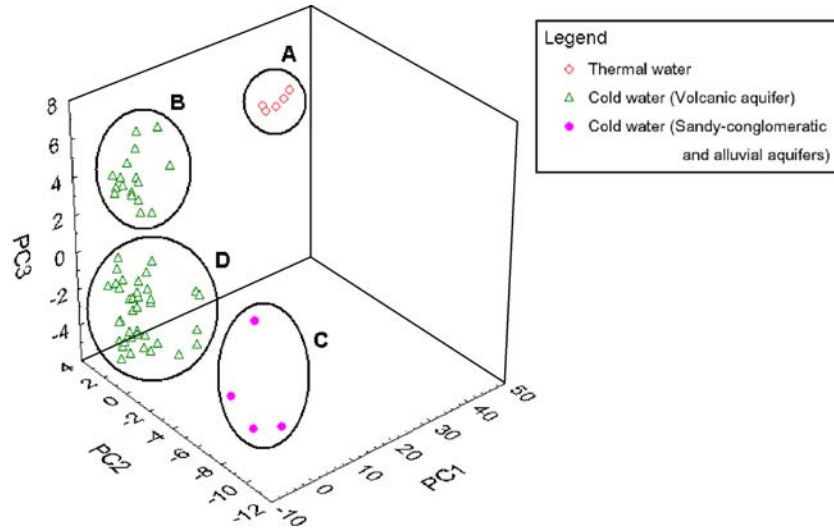


Fig. 6 Scatterplot of PCA scores (*PC1*, *PC2*, and *PC3*). Group A: thermal waters; group B: cold waters of the volcanic aquifer with relatively high concentrations of As, B, F⁻, and/or U; group C: cold waters of the Quaternary sedimentary aquifer with relatively high concentrations of Ca²⁺, HCO₃⁻, Cl⁻, and EC; group D: cold waters of the volcanic aquifer without combinations of extreme values for two or more variables

(Fig. 7). In the wide north-eastern zone, the wells and springs sampled correspond mainly to the basal and perched volcanic aquifers and secondly to sandy-conglomeratic and alluvial aquifers overlying the low-perme-

ability Pliocene-Pleistocene sedimentary rocks (Fig. 3). The waters of the volcanic aquifers mainly belong to group D, whereas those of the sandy-conglomeratic and alluvial aquifers comprise group C. The wells of the

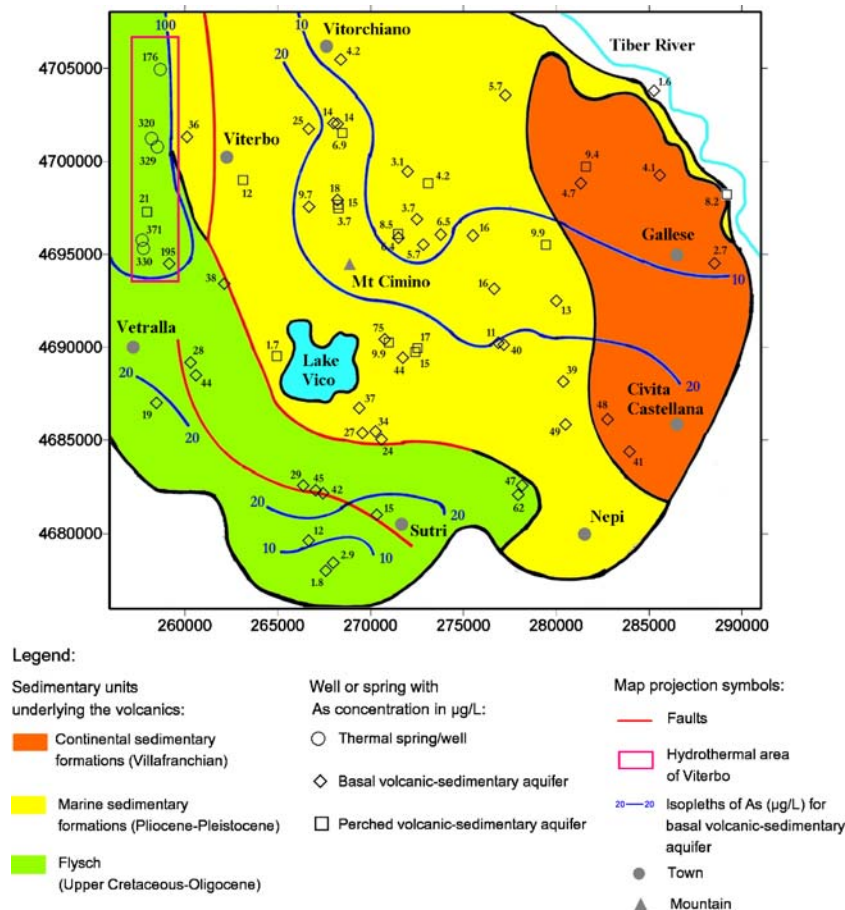


Fig. 7 Distribution and structure of sedimentary units underlying volcanics (modified from Baldi et al. 1974) and arsenic distribution in groundwater

south-eastern zone with low arsenic concentrations (<20 µg/L in Fig. 7) are characterized by waters belonging to group D and show a relatively reduced thickness of basal volcanic aquifers overlaying the Upper Cretaceous-Oligocene Flysch (Fig. 3).

Considering all the wells from volcanic and sedimentary aquifers, a strict and unequivocal correlation between arsenic concentration and depth was not found. In the zone where the arsenic content in the basal volcanic aquifer is above 20 µg/L, relatively lower concentrations occur in the perched aquifers, and the concentrations increase in the wells located near the faults (Fig. 3). Considering the aquifer formations, excluding the thermal waters, a wide variability in the arsenic concentration and higher values characterize the Vico Volcano products as detailed in Fig. 4.

Discussion

Hydrochemical data from this study, interpreted with reference to the specific geological and hydrogeological environments, highlight that the arsenic contents in groundwater are closely connected with the hydrothermal processes involving the volcanic region. The strong correlation of arsenic with temperature (Table 2 and Fig. 4) is direct evidence that the deep-rising fluids of the active hydrothermal system control the arsenic distribution in groundwater, as verified in other volcanic areas of central and southern Italy (Cremisini et al. 1979; Dall'Aglio et al. 2001; Aiuppa et al. 2003). Typically the waters sampled from springs and deep wells falling within the Viterbo hydrothermal area (springs 1, 6, 12, and 26 and well 25 in Fig. 2) are characterized by negative values of Eh, high values of B and F⁻, positive or near-zero SI values for calcite, dolomite, and fluorite, and significant content of H₂S, similar to results from previous studies (Piscopo et al. 2006). Altogether, these hydrochemical features agree with a model involving supply of this group of sites by reducing groundwater rising from a deep and confined aquifer, i.e. Triassic-Palaeogene carbonate rocks (Fig. 8).

The spatial distribution of the arsenic confirms that the maximum concentrations correspond to the springs and wells located where the deep and confined aquifer is uplifted under a reduced thickness of the semiconfining layer (i.e. the fractured and faulted Upper Cretaceous-Oligocene Flysch). In this area, the cold waters of the shallow volcanic aquifer show high arsenic content, as was seen in the deep well 33, which penetrates only the basal unconfined aquifer of the volcanites (Figs. 3 and 7). In addition, the water from this well is the only one among the cold waters characterized by a positive SI value for fluorite. This positive value is due to the mixing of the volcanic groundwater with deep-rising fluids, which are a consequence of the vertical hydraulic gradient existing through the semiconfining layer that controls the flow from the deep and confined aquifer towards the shallow and unconfined volcanic aquifer (Fig. 8).

The distribution of arsenic in the volcanic aquifer seems to also be influenced by the hydrostratigraphy and structural setting of the area. The values of arsenic between 20 and 100 µg/L found for the basal aquifer along the strip extending from the hydrothermal area towards the SE can be interpreted considering the influence of the rising groundwater from the geothermal system and horizontal flow directions of groundwater. The shape of the strip is consistent with the NW–SE orientations of faults that subdivide the deep structures and with that of the graben where the Vico Volcano activity developed (Fig. 7). In addition, the northern boundary of the strip coincides with one of the main groundwater divides of the basal volcanic aquifer (compare Figs. 2 and 7). In the eastern sector of the strip, where the substratum of the volcanic and sandy-conglomeratic aquifers is made up of the low-permeability Pliocene-Pleistocene sedimentary rocks, the relatively high concentration of arsenic can be related to the lateral inflow from the other sectors, where mixing of deep-rising fluids occurs. In the area with arsenic concentrations above 20 µg/L, the mixing of waters of the volcanic aquifer with the deep-rising fluids is corroborated by a relative decrease of the trace elements in the perched aquifers and a relative increase in the wells and springs located near the faults (Figs. 3 and 7).

In the north-eastern zone of the studied system, the low concentration of arsenic (generally less than 10 µg/L) can be related to the separation of the deep-rising fluids from the groundwater flow in the volcanic aquifer. The arched groundwater divide located in this zone isolates an aquifer sector where the groundwater is only recharged by infiltration on the northern slope of volcanic area (Fig. 2), where the low-permeability Pliocene-Pleistocene sedimentary rocks form a thick natural barrier to the upflow from the geothermal system (Fig. 8). Oxidizing conditions characterize the unconfined volcanic aquifer, and the arsenic concentration depends slightly on the groundwater depth, with the perched and basal aquifers being equally affected by significant arsenic concentrations, though with values less than 10 µg/L (Fig. 7). The lower concentrations found in the wells that were mainly influenced by circulation in the Quaternary sedimentary aquifer (wells 4, 15, and 34 in Fig. 2) highlight that the volcanic rocks are a mineralogical source for the background arsenic concentration in the other water points in this zone and that arsenic release depends on the time of the water–rock interaction. This may explain the lower arsenic concentrations for volcanic waters found in the wells of the southern zone of the system (values less than 10 µg/L in Fig. 7). For these wells, the groundwater may have had a short path in a portion of the thin volcanic aquifer isolated by lateral groundwater inflow from other sectors (Fig. 2) and falling in an area where the volcanic basement is composed of a considerable thickness of unfaulted Upper Cretaceous-Oligocene Flysch (e.g. well 65 in Fig. 3).

Even if the data appear to highlight a higher arsenic content for the aquifer portions made up of the Vico

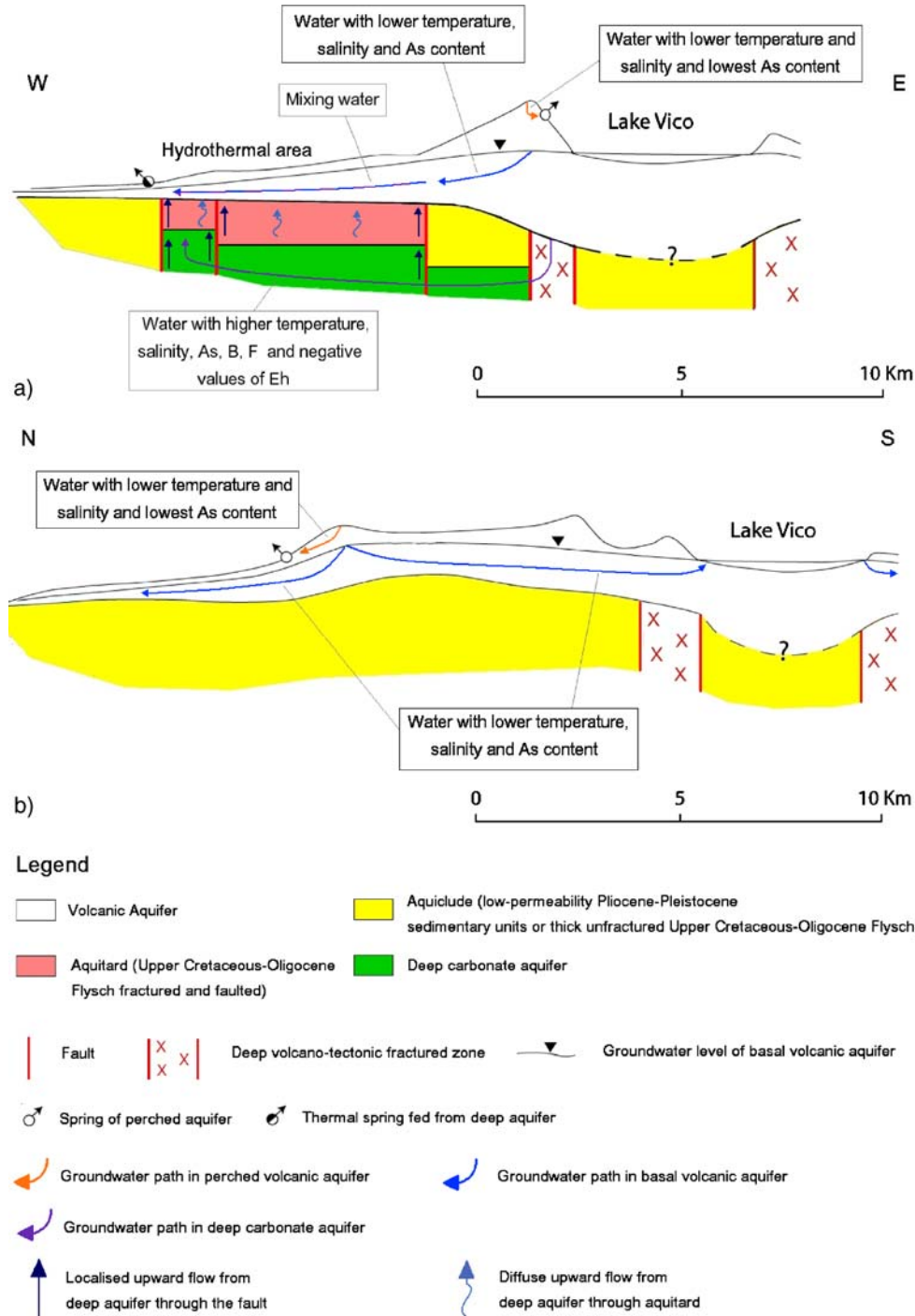


Fig. 8 Conceptual model showing the different flow paths in the volcanic and deep aquifers, and correlated occurrence of As in groundwater in response to hydrostratigraphy and structural setting of the Cimino-Vico volcanic area. **a** Cross-section through the hydrothermal area of Viterbo in the western zone of the Cimino-Vico system. **b** Cross-section through the north-eastern zone of the Cimino-Vico system

volcanites compared with those composed of the Cimino volcanites (Fig. 4), further studies are necessary to verify the influence of the different rock compositions. It must be considered that the volcanites of the Vico and Cimino complexes differ from one another in composition, age, porosity, and hydraulic conductivity. At present, it is clear that the hydrothermal processes involving the area are

connected to the more recent volcano-tectonic structures such as those where Vico Volcano developed.

A contribution due to the oxidative dissolution of arsenic-bearing sulphides could take place even if the water pH values (for most of the samples ≥ 7), the minor correlation of As vs SO_4^{2-} in the cold waters, and the non-correlation of As vs Fe do not allow this to be defined as a

main source. In addition, desorption from iron and manganese oxides could contribute to arsenic occurrence; however, despite the sampled waters being well correlated with competing anions and oxyanions (B, F, HCO_3^-), the measured pH values and the minor correlations of As with Fe and Mn did not allow for assessment of whether desorption is a significant process.

Even if the current data are not sufficient to describe the role of mineral phase dissolution on the water chemistry, the relation found between As and aquifer formation supports the hypothesis that the interaction with the volcanic rocks is at least partly involved in the arsenic distribution in groundwater, as it is in other volcanic areas (e.g. Welch et al. 1988). Altogether, the deep-rising fluids can be identified as the main source of arsenic in groundwater of the volcanic area as schematically reported in the conceptual model of Fig. 8. Further investigations are necessary in order to understand the arsenic input relative to the water–rock interaction and to judge its effects.

Conclusions

The occurrence of arsenic in groundwater of the Cimino-Vico volcanic area is mainly connected with the deep-rising fluids that characterize the active hydrothermal system. The highest arsenic concentrations (from 180 to 370 $\mu\text{g/L}$) were found in the thermal springs and wells (temperatures from 50 to 60°C) fed from relatively deep groundwater flow in the substratum of the volcanic aquifer. In the shallow volcanic aquifer, the distribution of arsenic in the groundwater is related to the local hydrostratigraphy, structural setting, and horizontal flow direction. Where the volcanic aquifer is open to the upward flow through the fractured, semiconfining Upper Cretaceous-Oligocene Flysch, relatively high arsenic concentrations (from 20 to 100 $\mu\text{g/L}$) were found. This is a consequence of mixing between deep groundwater and recharge by infiltration in the volcanic aquifer. An increase of arsenic in groundwater of the volcanic aquifer occurs in these hydrostratigraphical conditions, especially around the deep faulted zones. Where the volcanic aquifer is recharged only by infiltration and the aquifer base is sealed by a high thickness of low-permeability Pliocene-Pleistocene sedimentary rocks (and/or low-fractured Upper Cretaceous-Oligocene Flysch), arsenic concentrations less than 10 $\mu\text{g/L}$ were found. Relatively high arsenic concentrations were also found in these hydrostratigraphical conditions, but only where influence of groundwater inflow coming from the mixing zone occurs.

Some suggestions can be made from the study for management of the groundwater in the volcanic aquifer, which is naturally contaminated locally with arsenic (and sometimes also with fluoride), by taking into account a precautionary principle. At present, the groundwater resources of the volcanic and sedimentary aquifers supply the local demand of drinking water (about 150,000 inhabitants) and agricultural activity through numerous

wells and springs, located mainly based on proximity considerations for the users and on rate of flow. A new approach to groundwater management has been implemented to contain the impact on human health. Certainly, a more thorough geochemical mapping of the aquifers in the area would be a useful tool for a more accurate management of the water resources. Specifically, the nature and structure of the substratum of the volcanic aquifer must be included among the criteria to identify the location and manner of the groundwater withdrawals. Hydrothermal areas and faulted zones in the units underlying the volcanic aquifer represent the more vulnerable situations for the pumping for drinking water. Around these more vulnerable zones, it should always be verified that the pumping effects on the horizontal and vertical flow contain the mixing between the relatively shallow and deeper groundwater units.

Acknowledgements The authors would like to thank Marco Albano, Francesca Lotti and Paolo Proietti[†] for their assistance in the preparation of figures and in the sampling. The authors also express their gratitude to the managing and associate editors and two reviewers for constructive comments and suggestions for the enhancement of the manuscript.

References

- Aiuppa A, D'Alessandro W, Federico C, Palumbo B, Valenza M (2003) The aquatic geochemistry of arsenic in volcanic groundwater from southern Italy. *Appl Geochem* 18:1283–1296
- Anawar HM, Akai J, Mostofa KMG, Saffiullah S, Tareq SM (2002) Arsenic poisoning in groundwater: health risk and geochemical sources in Bangladesh. *Environ Int* 27:597–604
- Appleton JD (1972) Petrogenesis of potassium rich lavas from the Roccamonfina volcano, Roman Region Italy. *J Petrol* 13:425–456
- Baiocchi A, Dragoni W, Lotti F, Luzzi G, Piscopo V (2006) Outline of the hydrogeology of the Cimino and Vico volcanic area and of the interaction between groundwater and Lake Vico (Lazio Region, central Italy). *Boll Soc Geol Ital* 125:187–202
- Baldi P, Decandia FA, Lazzarotto A, Calamai A (1974) Studio geologico del substrato della copertura vulcanica laziale nella zona dei laghi di Bolsena, Vico e Bracciano [Geological study of the volcanites substratum in the Latium Region around the lakes Bolsena, Vico and Bracciano]. *Mem Soc Geol Ital* 13:575–606
- Ballantyne JM, Moore JN (1988) Arsenic geochemistry in geothermal systems. *Geochim Cosmochim Acta* 52:475–483
- Beccaluna L, Di Girolamo P, Serri G (1991) Petrogenesis and tectonic setting of the Roman Volcanic Province, Italy. *Lithos* 26:191–221
- Bertagnini A, Sbrana A (1986) Il vulcano di Vico: stratigrafia del complesso vulcanico e sequenze eruttive delle formazioni piroclastiche [The Vico Volcano: stratigraphy of the volcanic complex and sequence of the eruptions of the pyroclastic units]. *Mem Soc Geol Ital* 35:699–713
- Bhattacharyya R, Chatterjee D, Nath B, Jana J, Jacks G, Vahter M (2003) High arsenic groundwater: mobilization, metabolism and mitigation: an overview in the Bengal Delta Plain. *Mol Cell Biochem* 253:347–355
- Boni C, Bono P, Capelli G (1986) Schema idrogeologico dell'Italia centrale [Hydrogeological scheme of central Italy]. *Mem Soc Geol Ital* 35:991–1012
- Buonasorte G, Carbone MG, Conti MA (1991) Il substrato plio-pleistocenico delle vulcaniti sabatine: considerazioni stratigrafiche e paleoambientali [The Plio-Pleistocene substratum of the Sabatini volcanites: some stratigraphic and paleogeographic remarks]. *Boll Soc Geol Ital* 110:35–40

- Capelli G, Mazza R, Gazzetti C (2005) Strumenti e strategie per la tutela e l'uso compatibile della risorsa idrica del Lazio: gli acquiferi vulcanici [Tools and strategies to the safeguard and sustainable management of water resource in Lazio: the volcanic aquifers]. Pitagora, Bologna, Italy
- Čavar S, Klačec T, Grubešić RJ, Valek M (2005) High exposure to arsenic from drinking water at several localities in eastern Croatia. *Sci Total Environ* 339:277–282
- Charlet L, Polya DA (2006) Arsenic in shallow, reducing groundwaters in southern Asia: an environmental health disaster. *Elements* 2:91–96
- Corticelli S, Peccerillo A (1992) Petrology and geochemistry of potassic and ultrapotassic volcanism in central Italy: petrogenesis and inferences on the evolution of the mantle sources. *Lithos* 28:221–240
- Cremisini C, Dall'Aglio M, Ghiara E (1979) Arsenic in Italian rivers and in some cold and thermal spring. In: Proc. of Int. Conference on Management and Control of Heavy Metals in the Environment, Imperial College, London, 18–21 September 1979, pp 341–344
- Dall'Aglio M, Giuliano G, Amicizia D, Andrenelli MC, Cicioni GB, Mastroianni D, Sepicacchi L, Tersigni S (2001) Assessing drinking water quality in Northern Latium by trace elements analysis. In: Cidu R (ed.) Proc. of the 10th Int. Symp. on Water-Rock Interaction, Villasimius, Italy, June 2001, pp 1063–1066
- EC Directive (1998) Council Directive 98/83/EC of 3 November 1998 on the quality of water intended for human consumption. European Commission, Brussels
- Farnham IM, Stetzenbach KJ, Singh AK, Johannesson KH (2000) Deciphering groundwater flow systems in Oasis Valley, Nevada, using trace element chemistry, multivariate statistics, and geographical information system. *Math Geol* 32:943–968
- Farnham IM, Johannesson KH, Singh AK, Hodge VF, Stetzenbach KJ (2003) Factor analytical approaches for evaluating groundwater trace element chemistry data. *Anal Chim Acta* 490:123–138
- Fitzpatrick ML, Long DT, Pijanowski BC (2007) Exploring the effects of urban and agricultural land use on surface water chemistry, across a regional watershed, using multivariate statistics. *Appl Geochem* 22:1825–1840
- Funicello R, Locardi E, Lombardi G, Parotto M (1977) The main volcanic groups of Latium: relations between structural evolution and petrogenesis. *Geol Rom* 15:279–300
- Gómez JJ, Lillo J, Sahún B (2006) Naturally occurring arsenic in groundwater and identification of the geochemical sources in the Duero Cenozoic Basin, Spain. *Environ Geol* 50:1151–1170
- Hughes MF (2002) Arsenic toxicity and potential mechanisms of action. *Toxicol Lett* 133:1–16
- Jain CK, Ali I (2000) Arsenic: occurrence, toxicity and speciation techniques. *Water Res* 34:4304–4312
- Karim MM (2000) Arsenic in groundwater and health problems in Bangladesh. *Water Res* 34:304–310
- Kelepertsis A, Alexakis D, Skordas K (2006) Arsenic, antimony and other toxic elements in the drinking water of Eastern Thessaly in Greece and its possible effects on human health. *Environ Geol* 50:76–84
- Kim MJ, Nriagu J, Haack S (2002) Arsenic species and chemistry in groundwater of the southeast Michigan. *Environ Pollut* 120:379–390
- La Torre P, Nannini R, Sollevanti F (1981) Geothermal exploration in central Italy: geophysical survey in Cimino Range area. In: 43th Meeting European Association of Exploration Geophysicists, Venice, 26–29 May 1981
- Lardini D, Nappi G (1987) I cicli eruttivi del complesso vulcanico Cimino [The eruptive phases of the Cimino volcanic complex]. *Rend Soc Ital Mineral Petrol* 42:141–153
- Locardi E (1965) Tipi di ignimbrite di magmi mediterranei: le ignimbrite del vulcano di Vico [Types of ignimbrite eruptions of Mediterranean magma: ignimbrites of Vico Vulcano]. *Atti Soc Toscana Sci Natur* 72:53–173
- Locardi E (1967) Uranium and Thorium in the volcanic processes. *Bull Volcanol* 31:235–260
- Locardi E (1973) Mineralizzazioni ad uranio in vulcaniti quaternarie del Lazio [Uranium mineralization of Quaternary volcanites in Latium Region]. *Boll Soc Geol Ital* 92:541–566
- Mandal BK, Suzuki KT (2002) Arsenic round the world: a review. *Talanta* 58:201235
- Mari GM, Giuliano G, Preziosi E, Petrangeli AB, Vivona R, Patera A, De Luca A, Barbiero G (2006) Carte di vulnerabilità finalizzate al monitoraggio dei corpi idrici sotterranei. Aspetti metodologici generali e prima sperimentazione nell'area centro-settentrionale della provincia di Roma [Vulnerability maps addressed to groundwater monitoring: general methods and first testing in the central-southern area of Rome Province]. *Mem Descrit Carta Geol It* 49:37–50
- Marinelli G (1975) Magma evolution in Italy. In: CH Squyres (ed) *Geology of Italy, The Earth Science Society of the Lybian Arab Rep.*, Tripoli, pp 165–219
- Mattias PP, Ventriglia V (1970) La regione vulcanica dei Monti Cimini e Sabatini [The volcanic region of the Cimini and Sabatini Mountains]. *Mem Soc Geol Ital* 9:331–384
- Meglin RR (1991) Examining large databases: a chemometric approach using principal component analysis. *J Chemom* 5:163–179
- Meliker JR, Franzblau A, Slotnick MJ, Nriagu JO (2006) Major contributors to inorganic arsenic intake in southeastern Michigan. *Int J Hyg Environ Health* 209:399–411
- Morin G, Calas G (2006) Arsenic in soils, mine tailings, and former industrial sites. *Elements* 2:97–101
- Nappi G, Valentini L, Mattioli M (2004) Ignimbritic deposits in central Italy: pyroclastic products of the Quaternary age and Etruscan footpaths. In: APAT (ed) 32nd International Geological Congress Florence Field Trip Guide Book P09, APAT, Rome, 32 pp
- Nordstrom DK (2002) Worldwide occurrences of arsenic in groundwater. *Science* 296:2143–2145
- Parkhurst DL, Appelo CAJ (1999) Users guide to PHREEQC: a computer program for speciation, batch-reaction, one-dimensional transport, and inverse geochemical modelling. *US Geol Surv Water Resour Invest Rep* 99-4259, 312 pp
- Peccerillo A, Manetti P (1985) The potassium alkaline volcanism of central-southern Italy: a review of the data relevant to petrogenesis and geodynamic significance. *Trans Geol Soc South Africa* 88:379–384
- Perini G, Corticelli S, Francalanci L (1997) Inferences of the volcanic history of the Vico volcano, Roman Magmatic Province, central Italy: stratigraphic, petrographic and geochemical data. *Min Petr Acta* XL:67–93
- Piscopo V, Barbieri M, Monetti V, Pagano G, Pistoni S, Ruggi E, Stanzione D (2006) Hydrogeology of thermal waters in Viterbo area, central Italy. *Hydrogeol J* 14:1508–1521
- Plant JA, Kinniburgh DG, Smedley PL, Fordyce FM, Klinck BA (2005) Arsenic and selenium. In: Lollar BS (ed) *Environmental geochemistry*. Elsevier-Pergamon, Oxford
- Rahman MM, Sengupta MK, Ahamed S, Chowdhury UK, Hossain MA, Das B, Lodh D, Saha KC, Pati S, Kaies I, Barua AK, Chakraborti D (2005) The magnitude of arsenic contamination in groundwater and its health effects to the inhabitants of the Jalangi: one of the 85 arsenic affected blocks in West Bengal, India. *Sci Total Environ* 338:189–200
- Reyment RA, Jvreskog KG (1996) *Applied factor analysis in the natural sciences*. Cambridge University Press, Cambridge, 383 pp
- Rossmann TG, Uddin AN, Burns FJ (2004) Evidence that arsenite acts as a cocarcinogen in skin cancer. *Toxicol Appl Pharmacol* 198:394–404
- Smedley PL, Kinniburgh DG (2002) A review of the source, behaviour and distribution of arsenic in natural waters. *Appl Geochem* 17:517–568
- Sollevanti F (1983) Geologic, volcanologic and tectonic setting of the Vico-Cimino area, Italy. *J Volcanol Geotherm Res* 17:203–217
- Stetzenbach KJ, Hodge VF, Guo C, Farnham IM, Johannesson KH (2001) Geochemical and statistical evidence of deep carbonate

- groundwater within overlying volcanic rock aquifers/aquitards of southern Nevada, USA. *J Hydrol* 243:254–271
- Tchounwou PB, Centeno JA, Patlolla AK (2004) Arsenic toxicity, mutagenesis, and carcinogenesis: a health risk assessment and management approach. *Mol Cell Biochem* 255:47–55
- Vivona R, Preziosi E, Madé B, Giuliano G (2007) Occurrence of minor toxic elements in volcanic-sedimentary aquifers: a case study in central Italy. *Hydrogeol J* 15:1183–1196
- Webster JG, Nordstrom DK (2003) Geothermal arsenic. In: Welch AH, Stollenwerk KG (eds) *Arsenic in ground water, geochemistry and occurrence*. Kluwer, Dordrecht, The Netherlands, pp 101–112
- Welch AH, Lico MS, Hughes JL (1988) Arsenic in ground water of the western United States. *Ground Water* 26:333–347
- Yoshida T, Yamauchi H, Sun GF (2004) Chronic health effects in people exposed to arsenic via the drinking water: dose-response relationships in review. *Toxic Appl Pharmacol* 198:243–252